Engineering alcohol tolerance in yeast
Felix H. Lam *et al.*
Science **346**, 71 (2014);
DOI: 10.1126/science.1257859

is no fundamental limit to the directionality: By setting the polarization of the excitation field orthogonal to the polarization of the fiber eigenmodes that copropagate into the left/right direction, unity directionality can always be realized (*22*). Moreover, at the inside of the waveguide, the quasi-linearly polarized guided modes of our silica nanofiber exhibit a perfectly circular polarization at two specific positions in the fiber transverse plane. Thus, a particle at such a position that is excited with circularly polarized light will couple light exclusively into one direction of the waveguide. Apart from their usefulness for optical signal processing and routing of light, our findings have important consequences for the interaction between atoms and light in evanescent fields (*27*, *28*) or strongly focused laser beams. Moreover, they may enable novel nanophotonic sensors that allow one to detect and identify, for example, scatterers with an intrinsic polarization asymmetry (*22*, *29*). In the course of preparing this manuscript, we became aware of two related theoretical works (*30*, *31*) discussing effects based on directional emission in photonic crystal waveguides.

REFERENCES AND NOTES

1. D. K. Gramotnev, S. I. Bozhevolnyi, *Nat. Photonics* **4**, 83–91 (2010).
2. O. Benson, *Nature* **480**, 193–199 (2011).
3. L. Tong, F. Zi, X. Guo, J. Lou, *Opt. Commun.* **285**, 4641–4647 (2012).
4. M. Onoda, S. Murakami, N. Nagaosa, *Phys. Rev. Lett.* **93**, 083901 (2004).
5. A. David, M. Babiker, *The Angular Momentum of Light* (Cambridge Univ. Press, Cambridge, 2012).
6. K. Klitzing, G. Dorda, M. Pepper, *Phys. Rev. Lett.* **45**, 494–497 (1980).
7. S. Murakami, N. Nagaosa, S.-C. Zhang, *Science* **301**, 1348–1351 (2003).
8. K. Y. Bliokh, A. Y. Bekshaev, F. Nori, *Nat. Commun.* **5**, 3300 (2014).
9. Y. Zhao, J. S. Edgar, G. D. M. Jeffries, D. McGloin, D. T. Chiu, *Phys. Rev. Lett.* **99**, 073901 (2007).
10. J. Korger *et al.*, *Phys. Rev. Lett.* **112**, 113902 (2014).
11. O. Hosten, P. Kwiat, *Science* **319**, 787–790 (2008).
12. K. Y. Bliokh, A. Niv, V. Kleiner, E. Hasman, *Nat. Photonics* **2**, 748–753 (2008).
13. K. Y. Bliokh, Y. Gorodetski, V. Kleiner, E. Hasman, *Phys. Rev. Lett.* **101**, 030404 (2008).
14. F. J. Rodríguez-Fortuño *et al.*, *Science* **340**, 328–330 (2013).
15. J. Lin *et al.*, *Science* **340**, 331–334 (2013).
16. P. V. Kapitanova *et al.*, *Nat. Commun.* **5**, 3226 (2014).
17. C. Junge, D. O'Shea, J. Volz, A. Rauschenbeutel, *Phys. Rev. Lett.* **110**, 213604 (2013).
18. M. J. Morrissey *et al.*, *Sensors (Basel Switzerland)* **13**, 10449–10481 (2013).
19. J. Fam Le Kien, *Opt. Commun.* **242**, 445 (2004).
20. K. Y. Bliokh, F. Nori, *Phys. Rev. A* **85**, 061801 (2012).
21. J. D. Jackson, *Classical Electrodynamics* (John Wiley & Sons, New York, 1998).
22. Materials and methods are available as supplementary materials on *Science* Online.
23. G. Brambilla, *J. Opt.* **12**, 043001 (2010).
24. V. Myroshnychenko *et al.*, *Chem. Soc. Rev.* **37**, 1792–1805 (2008).
25. T. Bauer, S. Orlov, U. Peschel, P. Banzer, G. Leuchs, *Nat. Photonics* **8**, 23–27 (2014).
26. P. W. Barber, S. C. Hill, *Light Scattering by Particles: Computational Methods*, vol. 2 (World Scientific, Hackensack, NJ, 1990).
27. E. Vetsch *et al.*, *Phys. Rev. Lett.* **104**, 203603 (2010).
28. A. Goban *et al.*, *Phys. Rev. Lett.* **109**, 033603 (2012).
29. R. Mitsch, C. Sayrin, B. Albrecht, P. Schneeweiss, A. Rauschenbeutel, http://arxiv.org/abs/1406.0896 (2014).
30. A. B. Young *et al.*, http://arxiv.org/abs/1406.0714 (2014).
31. I. Söllner, S. Mahmoodian, A. Javadi, P. Lodahl, http://arxiv.org/abs/1406.4295 (2014).

ACKNOWLEDGMENTS

We gratefully acknowledge financial support by the NanoSci-ERA network "NOIs" and the European Commission (IP Simulators and Interfaces with Quantum Systems, 600645). J.V. acknowledges support by the European Commission (Marie Curie Intra-European Fellowship grant 300392). The scanning electron microscope imaging has been carried out by use of facilities at the University Service Center for Transmission Electron Microscopy, Vienna University of Technology, Austria.

SUPPLEMENTARY MATERIALS

www.sciencemag.org/content/346/6205/67/suppl/DC1
Materials and Methods
References (*32*–*35*)

19 June 2014; accepted 26 August 2014
10.1126/science.1257671

BIOFUELS

Engineering alcohol tolerance in yeast

Felix H. Lam,[1,2] Adel Ghaderi,[1] Gerald R. Fink,[2]* Gregory Stephanopoulos[1]*

Ethanol toxicity in the yeast *Saccharomyces cerevisiae* limits titer and productivity in the industrial production of transportation bioethanol. We show that strengthening the opposing potassium and proton electrochemical membrane gradients is a mechanism that enhances general resistance to multiple alcohols. The elevation of extracellular potassium and pH physically bolsters these gradients, increasing tolerance to higher alcohols and ethanol fermentation in commercial and laboratory strains (including a xylose-fermenting strain) under industrial-like conditions. Production per cell remains largely unchanged, with improvements deriving from heightened population viability. Likewise, up-regulation of the potassium and proton pumps in the laboratory strain enhances performance to levels exceeding those of industrial strains. Although genetically complex, alcohol tolerance can thus be dominated by a single cellular process, one controlled by a major physicochemical component but amenable to biological augmentation.

The increased use of renewable transportation fuels such as bioethanol is an accepted strategy to combat global climate change (*1*). However, the toxicity of ethanol and other alcohols to the yeast *Saccharomyces cerevisiae* is a primary factor limiting titer and productivity in industrial production (*2*, *3*). Ethanol tolerance is a complex phenotype: Studies have shown that no single genetic modification is capable of eliciting greater resistance at high ethanol levels (*4*–*7*).

Because toxicity may arise from chemical perturbation of the plasma membrane, we surmised that the ionic composition of the culture medium could play a role in exacerbating or ameliorating this destabilization (*8*–*10*). Therefore, we added various salts to high–cell-density and high-glucose cultures mimicking industrial fermentation to ascertain their effects on ethanol production.

Monopotassium phosphate (K-P_i) added to standard yeast synthetic complete (YSC) medium induced the greatest improvement (fig. S1), an effect that we dissected into components deriving from elevated potassium (K^+) and pH. Specifically, when the pH of cultures containing elevated potassium chloride (KCl) was manually adjusted with potassium hydroxide (KOH) throughout the course of fermentation to match that of cultures containing elevated K-P_i, ethanol titers were statistically indistinguishable ($P = 0.09$ from a two-sample t test; $P \leq 7.6 \times 10^{-3}$ for other pairs) from one another (figs. S2 and S3). We also determined that KCl elicited a statistically higher improvement than sodium chloride (NaCl), and that supplementation with NaCl and sodium hydroxide, or with monosodium phosphate, demonstrated a distinguishable boost over NaCl alone ($P \leq 2 \times 10^{-4}$ from pairwise t tests). Thus, the greatest improvements in ethanol production derived specifically from the increase in K^+ concentration and the reduction in acidity of the fermentation medium.

Over the course of a 3-day culture, supplementation with KCl and KOH enhanced ethanol titer and volumetric productivity (grams of ethanol per volume per hour), two key benchmarks of fermentative performance (Fig. 1A). Additionally, compared with equimolar KCl or matched pH alone, the combination of K^+ supplementation and acidity reduction enabled the complete utilization of glucose and decreases in the synthesis of acetic acid and glycerol, two undesired byproducts of fermentation (fig. S4, A to D). Ethanol titers of 115 to 120 g/liter have been reported previously from S288C (*11*), the inbred laboratory strain we used that is known for its low ethanol resistance (*5*, *12*, *13*). However, these studies were typically conducted using chemically undefined ("rich") media. The 128 ± 0.7 (SD) g/liter concentrations we observed were achieved using a purely synthetic formulation, allowing us to identify and precisely control the environmental components that affect ethanol tolerance.

[1]Department of Chemical Engineering, Massachusetts Institute of Technology (MIT), Cambridge, MA, USA. [2]Whitehead Institute for Biomedical Research, Cambridge, MA, USA.
*Corresponding author. E-mail: gfink@wi.mit.edu (G.R.F.); gregstep@mit.edu (G.S.)

The boost in ethanol production from KCl and KOH supplementation did not arise simply from an increase in cell number but from an increase in cell tolerance. Specifically, the 80 ± 1.3% jump in titer (Fig. 1A) was accompanied only by an 11 ± 4.6% average higher cell density (Fig. 1B); therefore, cell growth alone could not explain the rise in output. This discrepancy, however, was resolved when we directly assessed the fractions of cells remaining alive throughout fermentation (fig. S5A) and discovered that the addition of KCl and KOH enhanced overall population viability (Fig. 1B and fig. S5B). This enhancement, furthermore, occurred despite the increase in toxicity imposed by higher accumulations of ethanol.

When we calculated specific productivities (rates of ethanol increase normalized by the live, rather than total, cell population), the values from KCl and KOH supplementation differed from the control by an average of 11 ± 7.5% (Fig. 1A). The fact that these differences account for a minor portion of the increase in titer suggests that elevated K^+ and pH act primarily not by affecting per-cell output but by boosting tolerance and the overall viable cell population. Additionally, these effects were fully observed in fermentations conducted in anaerobic bioreactors, demonstrating that these tolerance improvements do not depend on oxygen availability and can scale to higher-volume environments (fig. S6).

Because it is the viable cell population that is actively fermenting, final titers are governed by both the number of live cells and the length of time over which cells maintain viability against rising ethanol toxicity. The time integral of the viable cell population captures these two aspects and quantifies the overall impact of tolerance on ethanol production (fig. S5, B and C). Indeed, varying the concentration of supplemental KCl resulted in a dose-dependent increase of these time integrals; moreover, when these same additions were done at a higher pH, integrated viable population values were shifted upward correspondingly (Fig. 1C and fig. S7A). A strong linear relationship exists between the time integrals of viable cell density and final titers [goodness-of-fit (R^2) = 0.96; $P = 1.5 \times 10^{-7}$], demonstrating that the ability to endure toxicity is a principal determinant of ethanol output and the primary trait strengthened by KCl and KOH supplementation (Fig. 1D and fig. S7B).

The enhancements conferred by elevated K^+ and reduced acidity transcend genetic background and were elicited universally among a random sampling of industrial yeast strains. Those used in the production of biofuel ethanol in Brazil (PE-2) and the United States (Lasaffre Ethanol Red), and of sake wine in Japan (Kyokai No. 7), are typically the result of genetic selection efforts designed to isolate superior ethanol phenotypes (*13*–*15*). Consequently, all demonstrated distinctly higher ethanol output than S288C [10 ± 1% to 30 ± 1.2%] when grown in unmodified medium (Fig. 2A). However, when subjected to KCl and KOH supplementation, all strains responded with enhancements in tolerance that enabled the complete consumption of glucose (fig. S8) and titers of 116 ± 0.9 to 127 ± 1.6 g/liter. Under these conditions, S288C performed indistinguishably from the two industrial bioethanol strains ($P \geq 0.08$ from pairwise t tests). Thus, a strain traditionally deemed ethanol-sensitive is inherently capable—without genetic modification—of superior tolerance, indicating that K^+ supplementation and acidity reduction drive a process that can supersede advantages conferred by genetic adaptation.

These adjustments to the medium, furthermore, enhance fermentation from xylose, an important hemicellulosic sugar that cannot be consumed by

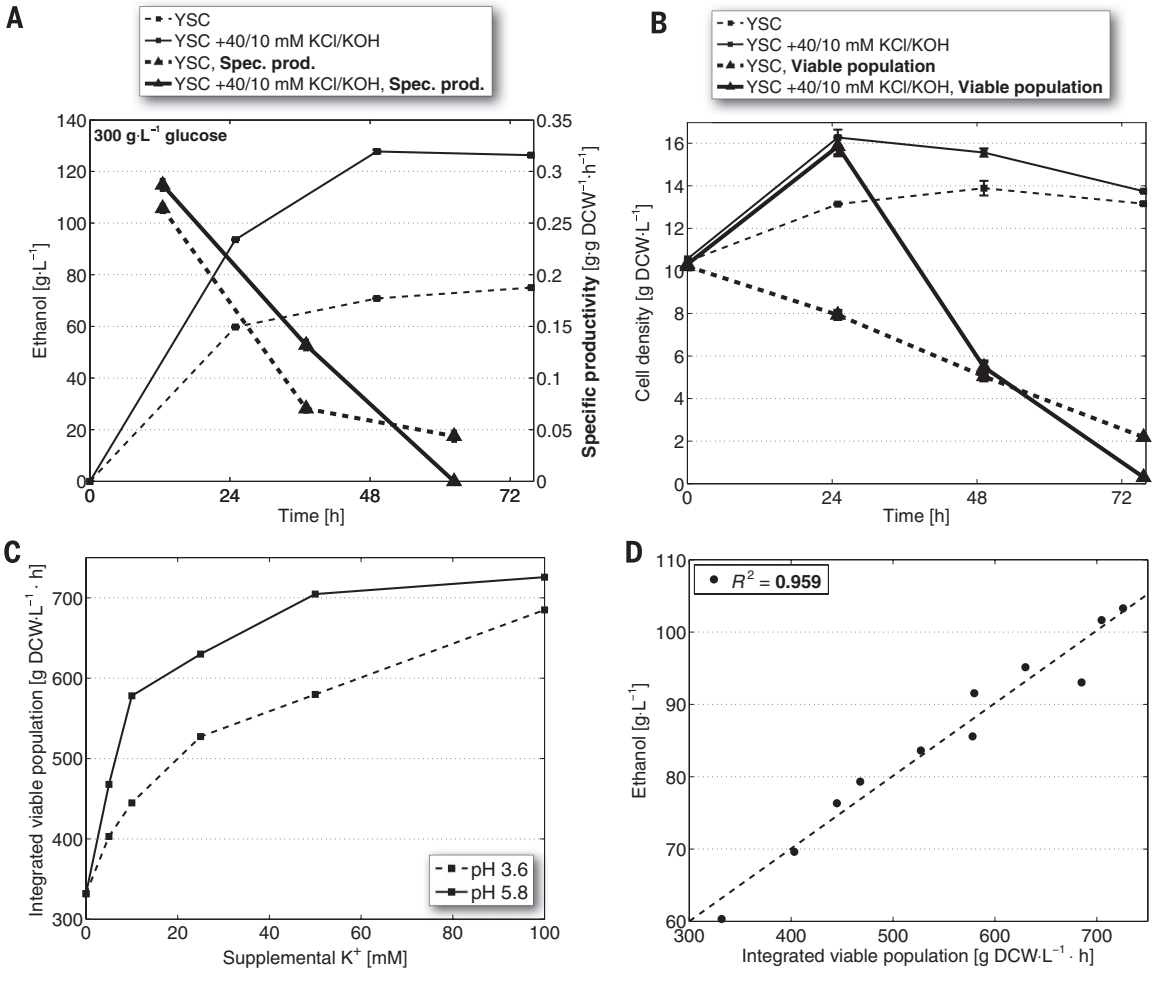

Fig. 1. Elevated extracellular potassium and pH enhance ethanol tolerance and production under high-glucose and high–cell-density conditions. (**A**) Ethanol titers (squares) and per-cell rates of production (triangles) from fermentations in unmodified YSC medium (dashed lines) or YSC supplemented with 40 mM KCl and 10 mM KOH (solid lines). Specific productivities are calculated from the mean viable population [thick lines from (B)] during each 24-hour period. DCW, dry cell weight. (**B**) Cell densities (DCW; thin squares) and the underlying viable populations (thick triangles) from the fermentations in (A). Data are mean ± SD from three biological replicates. (**C**) Net fermentation viability, expressed as time integrals of the viable cell population, as a function of potassium added to YSC in the form of KCl (pH 3.6), or 5 mM KOH + KCl (pH 5.8). (**D**) Time integral values from (C) regressed against their final ethanol titers.

standard strains of *S. cerevisiae*. In an engineered strain (*16*), 22 ± 0.9 g/liter ethanol was produced from unmodified medium containing 100 g/liter of xylose (Fig. 2A). When fermented with the addition of KCl and KOH, we observed a 54 ± 5.7% increase in titer, commensurate with the complete assimilation of xylose (fig. S8). Thus, K^+ supplementation and acidity reduction enhance tolerance in a manner impartial to the type of substrate.

The improvements conferred by elevated K^+ and pH generalize beyond synthetic media to chemically undefined broths, provided that such formulations do not already saturate for these effects. For example, in yeast extract peptone (YP) medium [~pH 6 and unknown concentrations of individual nutrients (*17*)], cells ferment all sugar, so no margin is available for improvement (fig. S9B). However, the impact of specific supplements can be assessed if the YP components are made limiting. Indeed, when YP was decreased to 30 or 3% while maintaining the same glucose concentration, supplementation with K^+ improved ethanol output, whereas additives shown to be fermentation-neutral (fig. S1) did not (fig. S9A). Using YP diluted to 20%, titers of 104 ± 0.8 g/liter were produced, whereas the addition of K^+ enhanced output 17 ± 2.5% (Fig. 2B). When pH was reduced from 6 to 3.7, production was concomitantly reduced 28 ± 0.8%. However, the subsequent addition of K^+ compensated for this decrease, restoring titers to 109 ± 1.8 g/liter. Thus, in media with undefined composition, extracellular K^+ and pH are also sufficient to quantitatively modulate ethanol performance.

To isolate the effects of KCl and KOH supplementation on tolerance from other fermentation variables (such as decreasing turgor pressure from glucose consumption), we subjected yeast to nonphysiological step increases in ethanol concentration and quantified the population fractions surviving after 80 min, a period much shorter than the length of fermentation but adequate for cell viability to be affected. In medium containing a subsistence amount of glucose that minimizes newly produced ethanol, elevated K^+ and pH enhanced viability in shocks up to 27% (vol/vol) when compared to cells stressed in unmodified conditions (Fig. 2C). Analogous experiments performed using high glucose (mimicking the osmotic conditions of high-gravity fermentation) and heightened K-P_i yielded a similar result, albeit at a lower range of ethanol concentrations (fig. S10A). These results indicate that the impact of elevated K^+ and reduced acidity is relatively immediate, does not require adaptation to ethanol accumulation over the course of days, and is capable of overcoming the combined stresses of high sugar and ethanol (*2*).

The boost in tolerance conferred by heightened K^+ and pH extends to higher alcohols capable of serving as unmodified substitutes for gasoline. Although at lower concentrations when compared to ethanol (reflecting their increased toxicity), we observed that viability is similarly enhanced when cells are shocked using step increases of isopropanol and isobutanol (Fig. 2, D and E, and fig. S10B). That the improvements are not unique to ethanol suggests that these adjustments to the medium augment a more general cellular process involved in alcohol resistance or membrane integrity.

Given the dominant effects exerted by extracellular K^+ and pH, we hypothesized that K^+ and proton (H^+) regulation may be a primary mechanism mediating the tolerance phenotype. Because opposing gradients of K^+ and H^+ ions are generated across the yeast plasma membrane by the K^+ importer *TRK1* and H^+ exporter *PMA1* (*18*, *19*), we surmised that genetic modifications of these adenosine triphosphate–dependent pumps, designed to perturb or strengthen these gradients, would produce corresponding effects to fermentative performance. Indeed, genetic deletions that debilitate K^+ import or H^+ export weakened ethanol output (fig. S11). Likewise, hyperactivation of *TRK1*, accomplished by deletions of *PPZ1* and *PPZ2* (*19*), generated an increase, yielding an 18 ± 1.6% (SD) improvement in titer over the wild type when cultured in unmodified medium (Fig. 3 and fig. S12A). Given the electroneutral codependence of the K^+ and H^+ gradients (*18*), we, furthermore, reasoned that up-regulation of *PMA1* alongside augmented *TRK1* would further enhance the ethanol phenotype; indeed, the combination increased titers by 27 ± 2.2% over the wild

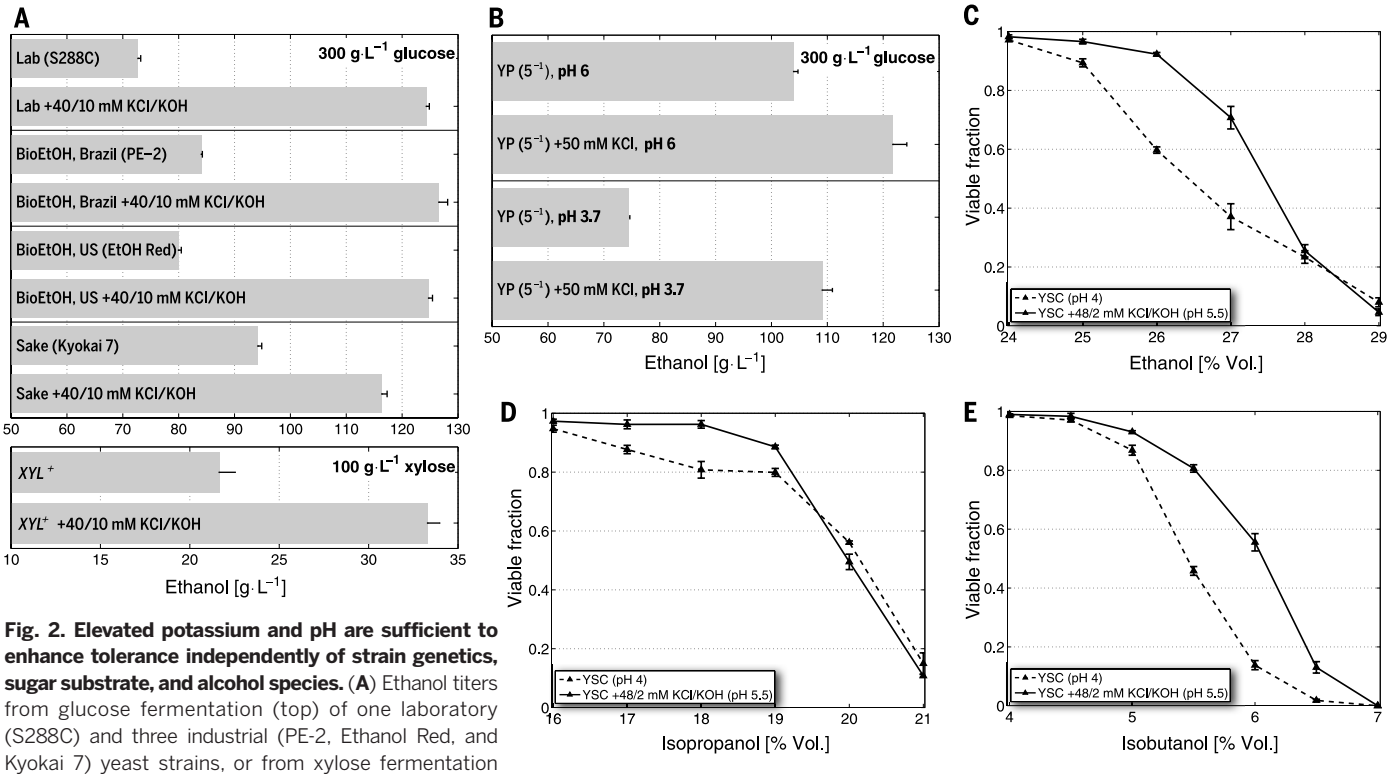

Fig. 2. Elevated potassium and pH are sufficient to enhance tolerance independently of strain genetics, sugar substrate, and alcohol species. (**A**) Ethanol titers from glucose fermentation (top) of one laboratory (S288C) and three industrial (PE-2, Ethanol Red, and Kyokai 7) yeast strains, or from xylose fermentation (bottom) of an engineered xylose strain, in unmodified YSC or YSC supplemented with 40 mM KCl and 10 mM KOH. (**B**) Titers from S288C cultured in 20% YP medium or medium supplemented with potassium, at pH 6 and 3.7. (**C**) Population fractions of S288C after transfer from overnight growth in unmodified YSC (dashed lines) or medium supplemented with 48 mM KCl and 2 mM KOH (solid lines) into media containing the indicated concentrations of ethanol. (**D** and **E**) Same as (C), but with step increases of isopropanol or isobutanol, respectively. All data are mean ± SD from three biological replicates.

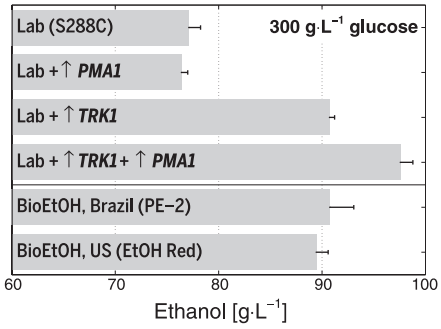

Fig. 3. Genetic augmentation of the plasma membrane potassium (*TRK1*) and proton (*PMA1*) pumps increases ethanol production to levels exceeding those of industrial strains. Shown are ethanol titers from a wild-type laboratory strain (S288C) transformed with empty overexpression plasmid, S288C transformed with a plasmid overexpressing *PMA1*, S288C containing hyperactivated *TRK1* (via deletions of *PPZ1* and *PPZ2*) and transformed with empty overexpression plasmid, the *TRK1* hyperactivated strain transformed with a plasmid overexpressing *PMA1*, and bioethanol production strains from Brazil (PE-2) and the United States (Ethanol Red), all cultured in unmodified YSC lacking uracil. Data are mean ± SD from three biological replicates.

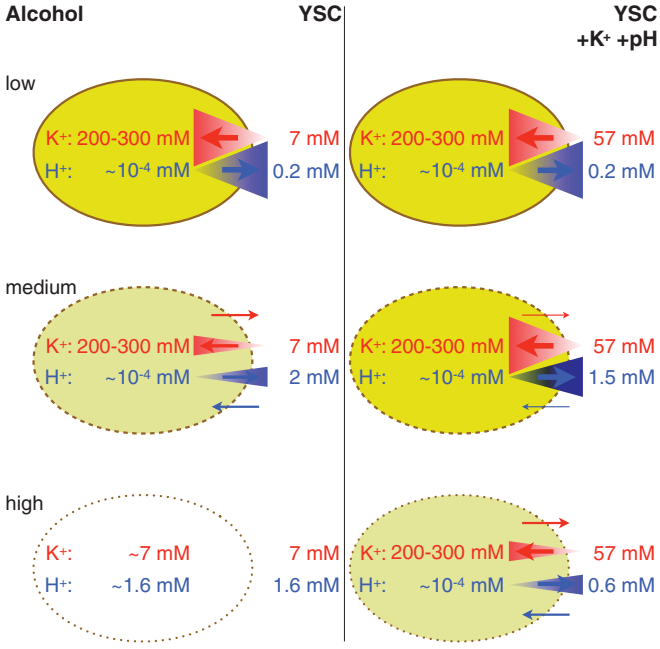

Fig. 4. Potential biophysical mechanism depicting how elevated potassium and pH counteract rising alcohol toxicity. In the absence of stress (top row), the opposing K^+ and H^+ pumps maximally maintain steep gradients of K^+ and H^+ across the plasma membrane. Rising alcohol levels perturb these gradients by permeabilizing the membrane and increasing ion leakage (middle row, left). Elevated potassium and pH, however, bolster the gradients by slowing rates of ion leakage (due to reduced concentration differences) and allowing transporters to pump against a less-precipitous differential (middle row, right). Therefore, the threshold alcohol concentration that collapses these gradients is raised, allowing cells to maintain viability at higher toxicity levels (bottom row). Red corresponds to K^+ and blue to H^+, the size of the triangles corresponds to concentration gradient steepness, and the thickness of the arrows corresponds to the magnitude of ion flux.

type. These improvements in output mirrored enhancements in net fermentation viability (fig. S12B), affirming the coupled nature of production and tolerance. Incidentally, overexpression of *PMA1* without hyperactivation of *TRK1* did not enhance ethanol performance (Fig. 3), supporting the proposed notion that K^+ uptake creates the dominant electromotive force, and H^+ efflux acts primarily as a response current (*19*).

Genetic augmentation of the K^+ and H^+ transporters increased ethanol titer of the laboratory strain to that surpassing the two bioethanol production strains (Fig. 3). These specific genetic modifications are, therefore, sufficient to create a superior phenotype that was previously available only through selection. That hyperactivation of *TRK1* alone is sufficient to match the titers of PE-2 and Ethanol Red, combined with the observation that these industrial strains respond to KCl and KOH supplementation, lends support to the possibility that polymorphisms enhancing the K^+ and H^+ gradients may be responsible for intrinsically higher ethanol tolerances (*20*).

Collectively, our results suggest a toxicity model in which alcohols attack viability not at threshold concentrations that solubilize lipid bilayers but at lower concentrations that increase the permeability of the plasma membrane and dissipate the cell's ionic membrane gradients. The observation that genetically unchanged cells can be made to tolerate higher ethanol concentrations by modulating extracellular K^+ and pH indicates that many observed tolerance thresholds (such as the sub–100 g/liter titers from unmodified medium) represent a physiological, rather than chemical, limit. Ethanol has been known to decrease intracellular pH in a dose-dependent fashion, demonstrating that its amphipathicity permeabilizes the plasma membrane to H^+ (and potentially other ions) (*8*, *21*). Furthermore, that the coupled K^+ and H^+ gradients comprise a dominant portion of the yeast electrical membrane potential, used to power many of the cell's exchange processes with the environment, hints that the cessation of nutrient and waste transport due to gradient dissipation may be a primary mode of cell death (*18*, *21*–*25*).

These ionic gradients are probably disrupted with increasing strength as ethanol accumulates during fermentation, requiring the cell to expend escalating amounts of energy to reestablish the steep separation of charges. Conditions that bolster the cell's efforts to maintain high concentrations of intracellular K^+ and low intracellular H^+ [estimated to be 200 to 300 mM and pH 7, respectively (*23*, *24*)] thus probably enhance tolerance by raising the threshold at which alcohols will collapse these gradients (Fig. 4). Physical reinforcements in the form of K^+ supplementation and acidity reduction generate the greatest improvements: Not only do higher concentrations of extracellular K^+ facilitate import (by potentially reducing the gradient from 36- to 4-fold, using the above estimates) and lower concentrations of extracellular H^+ facilitate export, the corresponding rates of ion leakage are decreased because of reduced concentration differences across the membrane. Likewise, genetic modifications strengthening the ion pump activities responsible for establishing the K^+ and H^+ gradients increase performance without alteration of the medium. However, that KCl and KOH supplementation confers larger improvements suggests that tolerance may contain a considerable physically driven component that ultimately constrains biological augmentation.

REFERENCES AND NOTES

1. A. L. Demain, *J. Indust. Microbiol. Biotechnol.* **36**, 319–332 (2009).
2. F. W. Bai, L. J. Chen, Z. Zhang, W. A. Anderson, M. Moo-Young, *J. Biotechnol.* **110**, 287–293 (2004).
3. G. Stephanopoulos, *Science* **315**, 801–804 (2007).
4. F. van Voorst, J. Houghton-Larsen, L. Jønson, M. C. Kielland-Brandt, A. Brandt, *Yeast* **23**, 351–359 (2006).
5. S. Swinnen *et al.*, *Genome Res.* **22**, 975–984 (2012).
6. D. Stanley, A. Bandara, S. Fraser, P. J. Chambers, G. A. Stanley, *J. Appl. Microbiol.* **109**, 13–24 (2010).
7. H. Alper, J. Moxley, E. Nevoigt, G. R. Fink, G. Stephanopoulos, *Science* **314**, 1565–1568 (2006).
8. A. Madeira *et al.*, *FEMS Yeast Res.* **10**, 252–258 (2010).
9. A. N. Dickey, R. Faller, *Biophys. J.* **92**, 2366–2376 (2007).
10. J. Chanda, S. Bandyopadhyay, *Langmuir* **22**, 3775–3781 (2006).
11. T. M. Pais *et al.*, *PLOS Genet.* **9**, e1003548 (2013).
12. J. A. Lewis, I. M. Elkon, M. A. McGee, A. J. Higbee, A. P. Gasch, *Genetics* **186**, 1197–1205 (2010).
13. J. L. Argueso *et al.*, *Genome Res.* **19**, 2258–2270 (2009).
14. T. Akao *et al.*, *DNA Res.* **18**, 423–434 (2011).
15. T. Katou, M. Namise, H. Kitagaki, T. Akao, H. Shimoi, *J. Biosci. Bioeng.* **107**, 383–393 (2009).
16. H. Zhou, J.-S. Cheng, B. L. Wang, G. R. Fink, G. Stephanopoulos, *Metab. Eng.* **14**, 611–622 (2012).
17. F. Sherman, *Methods Enzymol.* **350**, 3–41 (2002).
18. L. Yenush, S. Merchan, J. Holmes, R. Serrano, *Mol. Cell. Biol.* **25**, 8683–8692 (2005).
19. L. Yenush, J. M. Mulet, J. Ariño, R. Serrano, *EMBO J.* **21**, 920–929 (2002).
20. C. Reisser *et al.*, *G3* (2013).
21. C. P. Cartwright *et al.*, *Microbiology* **132**, 369–377 (1986).
22. R. Madrid, M. J. Gómez, J. Ramos, A. Rodríguez-Navarro, *J. Biol. Chem.* **273**, 14838–14844 (1998).

23. R. Orij, S. Brul, G. J. Smits, *Biochim. Biophys. Acta* **1810**, 933–944 (2011).
24. M. S. Cyert, C. C. Philpott, *Genetics* **193**, 677–713 (2013).
25. J. Horák, *Biochim. Biophys. Acta* **1331**, 41–79 (1997).

ACKNOWLEDGMENTS

We are grateful to present and former members of the Fink and Stephanopoulos labs for intellectual and technical guidance. Additionally, we thank V. Vyas and D. Pincus for critical commentary on the manuscript and Phibro for the gift of Lesaffre Ethanol Red. Support was provided by the MIT Energy Initiative and U.S. Department of Energy grant DE-SC0008744 to G.S. and National Institutes of Health grant R01-GM035010 to G.R.F. No competing financial interests impinged on this study. F.H.L., G.R.F., and G.S. are listed as co-inventors on a patent application filed by MIT and the Whitehead Institute. F.H.L., G.R.F., and G.S. designed all experiments and collaborated on the manuscript; A.G. conducted all bioreactor studies; and F.H.L. performed all other experiments, strain construction, and analysis of data. Supporting data are available in the supplementary materials.

SUPPLEMENTARY MATERIALS

www.sciencemag.org/content/346/6205/71/suppl/DC1
Materials and Methods
Supplementary Text
Figs. S1 to S13
Tables S1 to S3
References (*26*–*33*)
Database S1

24 June 2014; accepted 28 August 2014
10.1126/science.1257859

BIOFUELS

Altered sterol composition renders yeast thermotolerant

Luis Caspeta,[1]* Yun Chen,[1] Payam Ghiaci,[2] Amir Feizi,[1] Steen Buskov,[3] Björn M. Hallström,[4] Dina Petranovic,[1,2] Jens Nielsen[1,2,5]†

Ethanol production for use as a biofuel is mainly achieved through simultaneous saccharification and fermentation by yeast. Operating at ≥40°C would be beneficial in terms of increasing efficiency of the process and reducing costs, but yeast does not grow efficiently at those temperatures. We used adaptive laboratory evolution to select yeast strains with improved growth and ethanol production at ≥40°C. Sequencing of the whole genome, genome-wide gene expression, and metabolic-flux analyses revealed a change in sterol composition, from ergosterol to fecosterol, caused by mutations in the C-5 sterol desaturase gene, and increased expression of genes involved in sterol biosynthesis. Additionally, large chromosome III rearrangements and mutations in genes associated with DNA damage and respiration were found, but contributed less to the thermotolerant phenotype.

Microbial fermentation of biomass-derived feedstocks represents an attractive solution for production of sustainable liquid transportation fuels (*1*, *2*). About 100 billion liters of ethanol are produced annually by fermentation of mainly sugarcane saccharose and corn starch by the yeast *Saccharomyces cerevisiae* (*3*, *4*). There is also a growing interest in using this yeast for production of advanced biofuels with properties more similar to those of petroleum-derived fuels, and for using other biomass for fermentation, such as lignocellulose from residual biomass (*2*, *5*–*7*). The production of ethanol or advanced biofuels benefits greatly from fermentations at high temperature (≥40°C), because this reduces cooling costs and helps prevent contamination (*3*, *8*). High operating temperature also enables more efficient hydrolysis of the feedstock, thus leading to improved productivities in simultaneous saccharification and fermentation (*8*–*10*). In these processes, thermophilic enzymes and yeast are added simultaneously to ensure concurrent hydrolysis of starch or biomass into monosaccharides, and their further conversion to biofuels by yeast fermentation. However, temperatures ≥34°C seriously impair yeast viability and growth.

Thermotolerance in yeast *S. cerevisiae* can be induced by short-term exposure to nonlethal stress conditions including low pH, high osmolarity, elevated ethanol concentrations, and superoptimal temperatures (≥37°C) (*11*, *12*). The acquired thermal protection is, however, nonheritable and is attributable to induction of cellular responses including the accumulation of heat-shock proteins (Hsp) and/or trehalose, which can provoke cell cycle arrest at the G_1 phase, and low adenosine 3′,5′-monophosphate–protein kinase (cAMP-PK) activity concomitant with reduced glycolytic fluxes (*11*, *12*). Thus, adaptation due to the activation of the heat-shock response is not the most suitable strategy for biofuel production. Industrial thermotolerant yeast strains currently used for bioethanol production were selected in the production processes, where they were exposed to high temperatures for longer periods of time (*3*, *4*). These strains can grow and consume glucose faster at higher temperatures than strains that have just been adapted by stress induction. Although the industrial strains have been used globally for ethanol production, little is known about the genomics of the strains and what makes them thermotolerant (*4*).

We established three independent yeast populations from three individual clones of the haploid wild-type *S. cerevisiae* yeast strain CEN.PK113-7D, and we used adaptive laboratory evolution (ALE) to select thermotolerant strains that were extensively characterized (*13*).

Our ALE approach resulted in three parallel selections: Three clonal populations grew at 39.5 ± 0.3°C for more than 90 days, producing over 300 generations (Fig. 1A). After 326, 344, and 375 generations, the specific growth rate (μ) increased on average 1.57 ± 0.11 times in all three populations. We determined the specific growth rate of nine thermotolerant strains (TTSs), three randomly picked from each population (Fig. 1A). Seven TTSs had very similar growth kinetics at 40 ± 0.1°C under fully aerobic conditions (Fig. 1B). These strains grew on average 1.91 ± 0.12 times faster, consumed glucose on average 1.50 ± 0.2 times faster, and excreted ethanol and glycerol on average 1.6 ± 0.09 and 1.3 ± 0.08 times faster, respectively, than the parental strain (Fig. 1, B and C). The biomass yield on glucose increased by an average of 18 ± 0.5% (Fig. 1D).

We sequenced the genomes of the seven strains (TT11, TT12, TT13, TT21 TT22, TT31, and TT33) and performed whole-genome transcriptional profiling during exponential growth on glucose in bioreactors at 40 ± 0.1°C. Whole-genome sequencing revealed a total of 30 single-nucleotide variations (SNVs) in 18 genes (tables S1 and S2). The average number of SNVs per genome duplication was $1.9 \times 10^{-9} \pm 2.6 \times 10^{-10}$, and the average number of SNVs per 100 generations was 2.43 ± 0.3, which is higher than that reported for adaptation to other stresses (1.13 to 2.13 per 100 generations) (*14*). Most SNVs were detected in genes affecting membrane composition and structure, respiration, DNA repair, and replication (Fig. 2A). Nonsense mutations in the C-5 sterol desaturase gene *ERG3* were present in all lineages (table S2). Large genetic duplications were also found in five out of the seven strains. These consisted of two different types of segmental duplications of chromosome III (ChrIII), each found in strains isolated from two of the lineages (Fig. 2, B and C). It was previously reported that complete duplication of ChrIII in the diploid *S. cerevisiae* strains was selected during growth at 39°C, but this reported duplication was unstable and disappeared after 600 generations (*15*).

The three evolved yeast strains isolated from population 1, TT11, TT12, and TT13 all had a duplicated ChrIII region containing the *HCM1*, *RRT12*, *IMG1*, *IMG2*, *PER1*, and *YCR007* genes (fig. S1). A previous study showed that overexpression of these genes contributed to up to 23.5% of the thermotolerant phenotype (*15*). We did not find that duplications of some of these genes on ChrIII resulted in higher gene transcription,

[1]Novo Nordisk Foundation Center for Biosustainability, Chalmers University of Technology, SE-41296 Gothenburg, Sweden. [2]Department of Chemical and Biological Engineering, Chalmers Unversity of Technology, SE-41296 Gothenburg, Sweden. [3]Novozymes, Analytical Science, DK-4400 Kalundborg, Denmark. [4]Science for Life Laboratory, Royal Institute of Technology, SE-17121 Stockholm, Sweden. [5]Novo Nordisk Foundation Center for Biosustainability, DK-2970 Hørsholm, Denmark.
*Present address: Centro de Investigación en Biotecnología, Universidad Autónoma del Estado de Morelos, ME-62209 Morelos, México. †**Corresponding author: E-mail: nielsenj@chalmers.se**